Electronic Supplementary Information

Probing promoting effects of alkali cations on the reduction of CO at the aqueous electrolyte/copper interface

Charuni M. Gunathunge, Vincent J. Ovalle, and Matthias M. Waegele[*]

Department of Chemistry, Merkert Chemistry Center, Boston College, Chestnut Hill, MA 02467

E-mail: waegele@bc.edu

List of Figures

Experimental Procedures

Materials. NH_4F (40 wt.% in H_2O), HF (48 wt.%), Cs_2CO_3 (99.995%; trace metals basis), Li_2CO_3 (99.999%; trace metals basis), and Cu foil (99.8%; metals basis, 0.025 mm thick) were purchased from Fisher Scientific. $CuSO_4 \cdot 5H_2O$ (99.999%; trace metals basis), Na_2EDTA ($99.0 - 101.0\%$; ACS Reagent), 2,2-bipyridine ($\geq 99\%$; ReagentPlus), HCHO (35 wt.%; 10% methanol as stabilizer), NaOH (99.99%; trace metals basis), $KHCO_3$ ($\geq 99.95\%$; trace metal basis), and D_2O (99.9 atom %D) were purchased from Sigma Aldrich. Polycrystalline diamond pastes were purchased from South Bay Technologies (San Clemente, CA) or Electron Microscopy Sciences (Hatfield, PA). Ar (Ultra High Purity), CO (99.999%), CO_2 (5.0 research grade) were purchased from Air Gas. For all experiments, high purity water (18.2 $M\Omega$ cm) derived from Barnstead Nanopure Diamond system (APS Water Services; Lake Balboa, CA) was used.

Cu Thin Film Preparation. Polycrystalline copper films were electrolessly deposited onto the reflecting pane of a 60° Si prism (Pike Technologies; Madison WI). The Cu thin films were prepared by a chemical plating technique previously reported,[1-3] with slight modifications. The reflecting surface of the prism was sequentially polished with 6, 1, and 0.5 μm diamond pastes for 10, 15, and 10 min respectively. Remnants of polish were rubbed off with a wet Kim-wipe under the constant flow of Nanopure water for $5 - 10$ min. The crystal was then sonicated in water, acetone, and then water for 10, 5, and 5 min, respectively. The surface was then etched by immersion into aqueous 40 wt.% NH_4F (25°C) for 30 s. After rinsing with Nanopure water, the surface was then Cu-seeded with a 0.5 wt.% HF bath containing 750 μM $CuSO_4$ (25°C) for 1.5 min. The reflecting surface was rinsed with Nanopure water and immersed into a plating bath (0.25 M HCHO, 0.02 M $CuSO_4$, 20 mM Na_2EDTA, and 0.3 mM 2,2-bipyridine; pH=12; T=54$-$55°C) for 4 min. To electrically connect the thin film with the potentiostat, a ring of Cu foil was clamped between the circular edge of the film and a Viton O-ring sealing the electrochemical cell. After assembly of the cell, the resistance of the Cu film was measured to be $2 - 10$ Ω. Immediately following the assembly,

the copper film was covered in 4 ml of electrolyte. After purging the electrolyte with Ar at a flow rate of 5 sccm for 20 min, the film was treated with five cleaning voltammetric cycles from 0.09 to -0.48 V vs. SHE at a scan rate of 50 mV s^{-1} (Fig. S1 A). The potential was then linearly scanned to a potential of -0.38 V vs. SHE at 10 mV s^{-1} and the Cu film capacitance was determined using the method described below.

Thin Film Characterization. The roughness of the film was determined before and after each experiment by measuring the capacitance of the electrochemical double layer. The double layer capacitance was calculated from the charging currents determined from cyclic voltammograms recorded in the range of -0.38 to -0.48 V vs. SHE at scan rates of 20, 40, 60, 80, and 100 mV s^{-1} in either of Ar, CO or CO_2 saturated electrolytes (Fig. S1 B). Capacitance measurements reveal a film roughness factor of ≈ 10, in excellent agreement with previous studies that showed that the films are approximately 80 nm thick and consist of interconnected 100 nm crytallites.[1,2] The roughness of the films typically decreased by about $5 - 20\%$ following the spectroelectrochemical measurements. The current density was calculated by dividing the observed current by the geometric surface area of the Cu films (1.9 cm^2).

ATR-FTIR Measurements. When the potentiostat program was switched from the film characterization to the CV or kinetic experiment, the cell was kept at open circuit potential for less than 1 min. The Cu thin-film coated Si internal reflection element was interfaced with a customized PEEK electrochemical cell and coupled to a commercial ATR accessory (VeeMax III; Pike Technologies; Madison,WI). Spectra were recorded with a nitrogen-purged Bruker Vertex 70 FTIR spectrometer (Billerica, MA) equipped with a liquid nitrogen-cooled MCT detector (FTIR-16; Infrared Associates; Stuart, FL). The change in optical density was calculated according to $\Delta mOD = -10^3 \cdot \log(S/R)$, with S and R referring to the single beam sample spectrum and single beam reference spectrum, respectively. Schemes for the collection of spectra during CV and transient measurements are presented in Figs. S2 and S6, respectively.

Electrochemical Methods. All experiments were carried out in a single compartment electrochemical cell with a Ag/AgCl reference electrode (RE-5B 3 M NaCl; BASi Inc.; West Lafayette, IN) and a Au wire (99.999%; Alfa Aesar) as the counter electrode. The Ag/AgCl electrode was regularly calibrated against a saturated calomel electrode (CHI 150; CH Instruments Inc.; Austin, TX). The cell was cleaned in an acid solution (30 wt.% H_2SO_4, 30 wt.% HNO_3) for one hour followed by sonication in Nanopure water for one hour prior to each experiment. 85% of the cell resistance (typically between $2-25$ Ω) was compensated *in situ* with the VersaStat3 potentiostat (AMETEK; Berwyn, PA).

All measurements were carried out in either 0.1 M $MDCO_3$ or 0.05 M M_2CO_3 electrolyte solutions (M=Li, K, or Cs) in D_2O. 0.1 M bicarbonate solutions with Cs and Li cations were prepared by bubbling CO_2 at a rate of 10 sccm through solutions of 0.05 M Cs_2CO_3 or 0.05 M Li_2CO_3 for 1 hour. $KDCO_3$ was prepared through hydrogen-deuterium exchange by dissolving $KHCO_3$ in D_2O and subsequently evaporating the water. Using mass flow controllers (GE50A; MKS; Andover, MA), the electrolyte was purged with either CO or CO_2 gas at a constant flow (5 sccm) throughout the experiment. The pH* was measured before and after the experiment and was found to typically increase by about $\approx 0.1-0.2$ pH units during the course of a CV measurement in CO-purged electrolyte (pH* refers to the pH as measured with a pH meter in D_2O electrolytes.).
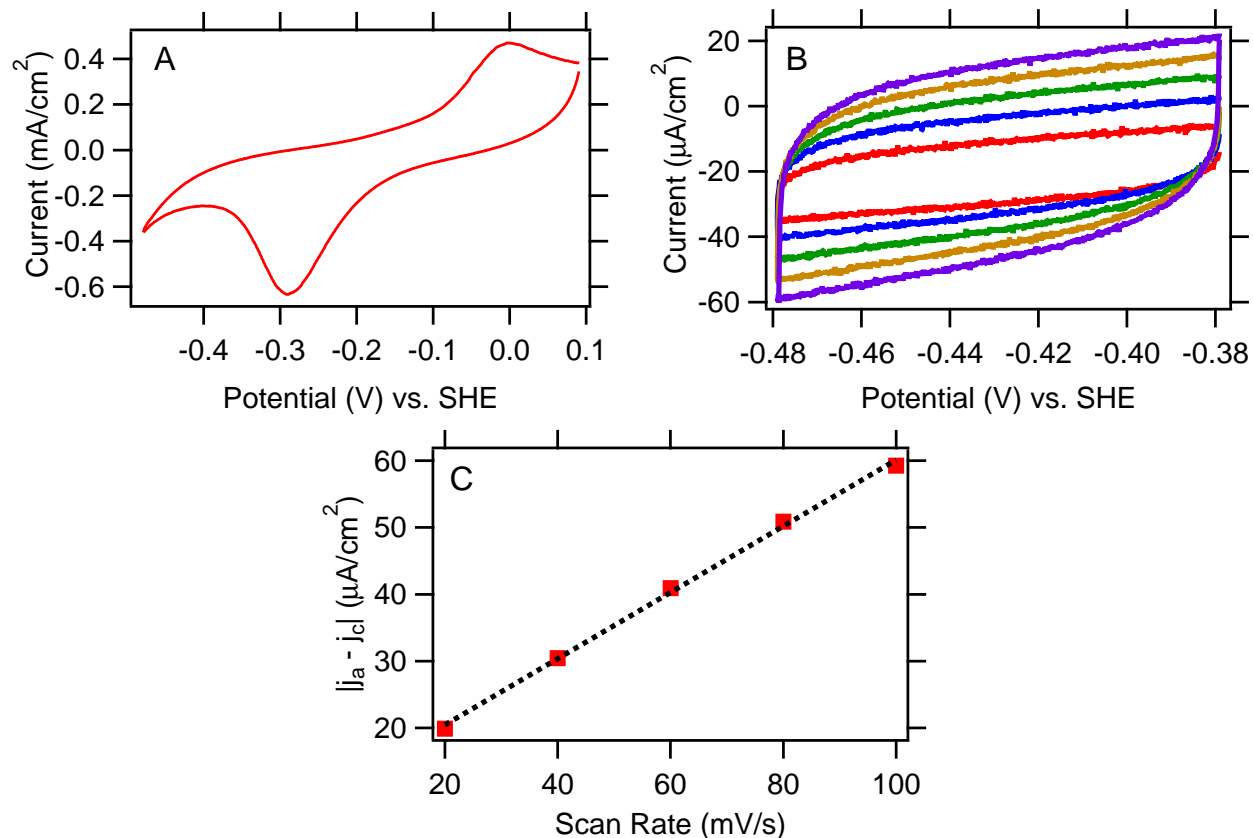
Fig. S 1: (A) Representative cyclic voltammogram obtained following four Cu film cleaning cycles from 0.09 to -0.48 V at a scan rate of 50 mV s^{-1} . (B) Representative CVs taken at scan rates of 20 (red), 40 (blue), 60 (green), 80 (yellow), and 100 mV s^{-1} (purple) to measure the double layer capacitance. (C) The double layer charging current vs. scan rate for the data shown in B (red squares) and the linear fit (black dotted line) to the data. The roughness of the film was calculated by dividing the slope of the line shown in graph C by a factor of two and a reference double layer capacitance value of 28 μF cm^{-2} for a smooth Cu surface.[4]

-0.38 V vs. SHE
20 min

Cyclic Voltammetry
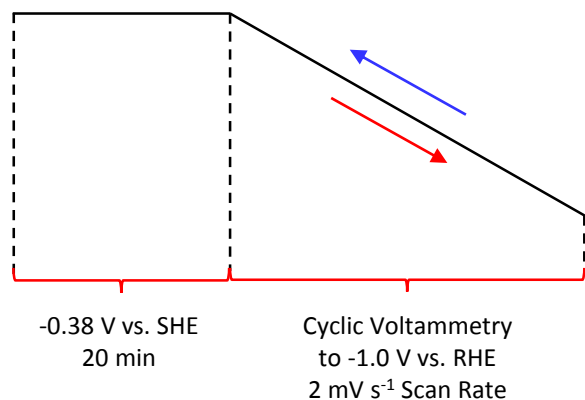to -1.0 V vs. RHE
2 mV s^{-1} Scan Rate

Fig. S 2: Cyclic voltammetric measurements. The potential was first held for 20 min while applying a reference potential of -0.38 V under CO or CO_2 purge, and then scanned to the turning potential of -1.0 V vs. RHE with a scan rate of 2 mV s^{-1}. The red arrow represents the cathodic (forward) scan, while the blue arrow represents the anodic (reverse) scan. IR spectra were concurrently acquired with a spectral resolution of 4 cm^{-1} in 4.6 s intervals. The scanner velocity was 40 kHz. An average of 19 spectra acquired just before the voltage ramp served as the reference single beam spectrum.
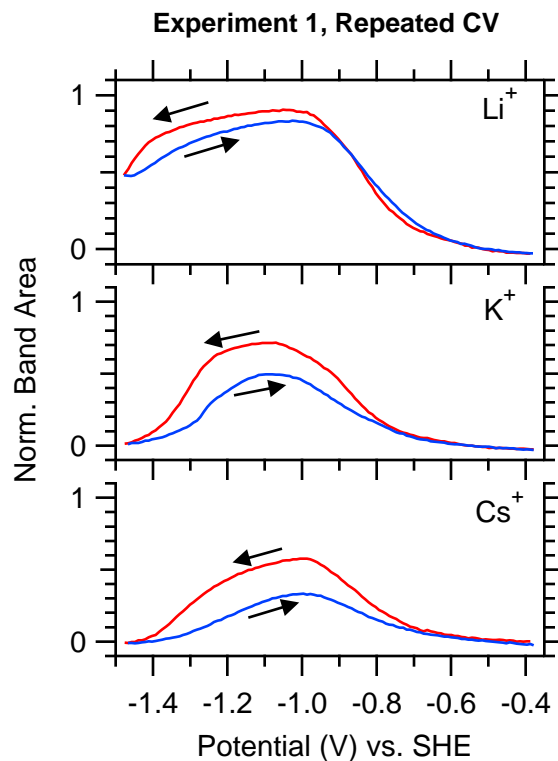
Fig. S 3: Normalized integrated band areas of linearly-bonded CO as a function of applied potential during the second CV cycle of the experiment shown in Fig. 2 of the main text. The normalization constants are 618, 728, and 587 mOD cm^{-1} for Li$^+$, K$^+$, and Cs$^+$, respectively. The normalization constants are the maxima of the integrated band areas of the cathodic scans of the first CVs (Fig. 2 of the main text).
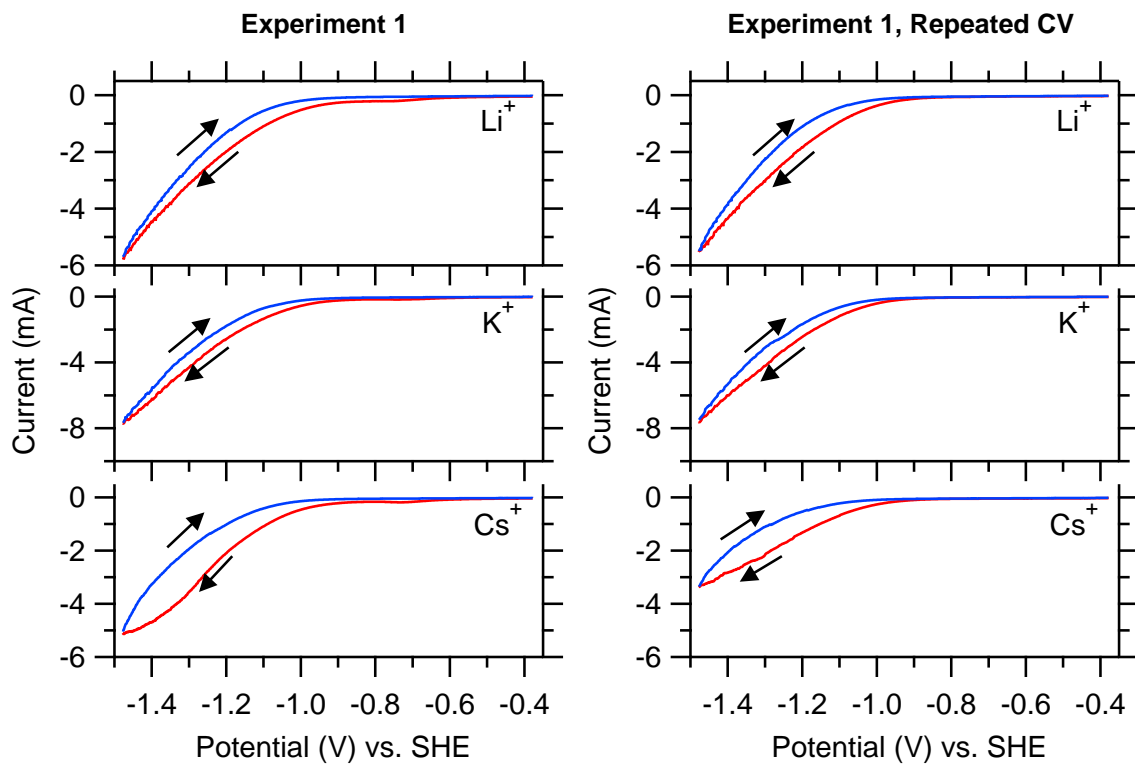
Fig. S 4: Cyclic voltammetric current-voltage curves for the data presented in Fig. 2 of the main text and Fig. S3.
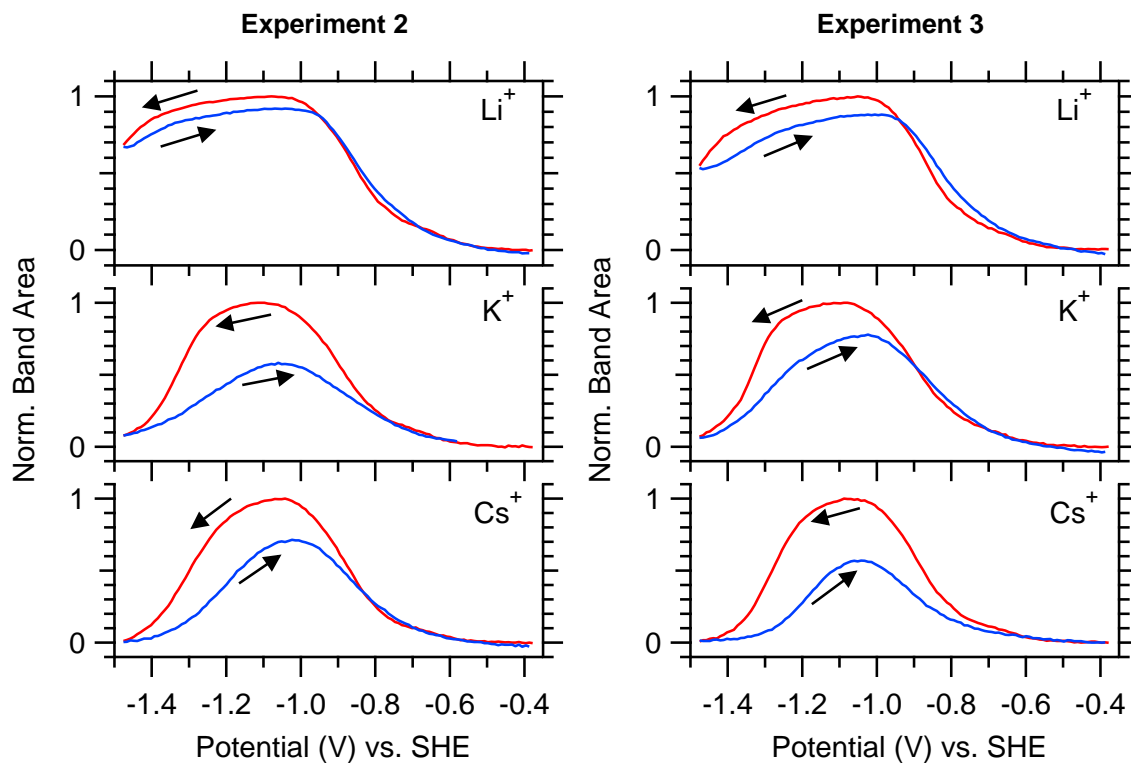
Fig. S 5: Normalized integrated band areas of linearly-bonded CO as a function of applied potential for two additional experiments for each cation in CO-saturated 0.1 M alkali metal bicarbonates as indicated. The normalization constants for Experiment 2 are 731, 463, and 364 mOD cm^{-1} for Li$^+$, K$^+$, and Cs$^+$, respectively. The normalization constants for Experiment 3 are 605, 478, and 482 mOD cm^{-1} for Li$^+$, K$^+$, and Cs$^+$, respectively.
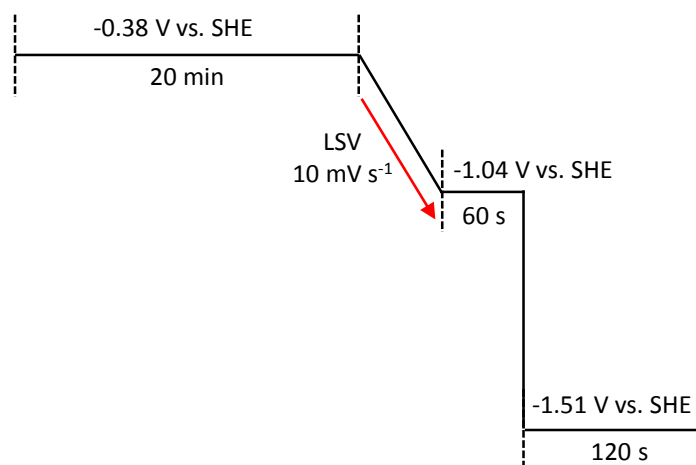
Fig. S 6: Transient measurements. The potential was held at -0.38 V for 20 min under CO purge. Then, the potential was scanned to the CO adsorption potential of -1.04 V, which was held for 60 s before the potential was jumped to -1.51 V. Spectra were collected throughout the experiment with a spectral resolution of 16 cm^{-1} at ≈ 52 ms intervals. The scanner velocity was 160 kHz. An average of 95 spectra acquired $\approx 1 - 2$ s before the potential jump served as the reference single beam spectrum.
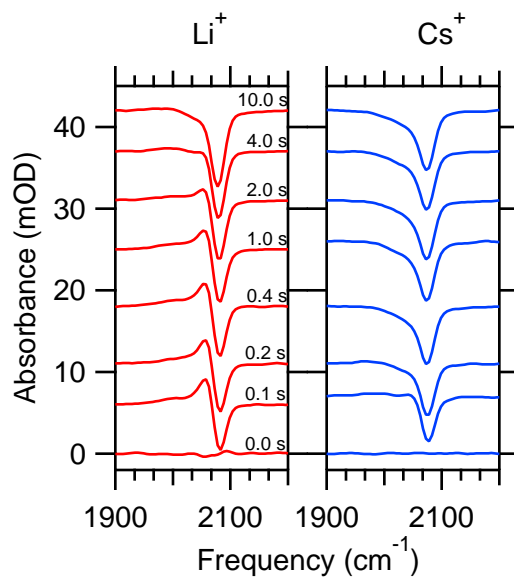
Fig. S 7: Representative transient CO spectra for Li^+- (red) and Cs^+- (blue) containing electrolytes a function of time for kinetic data presented in Fig. 3 of the main text. The numbers indicate the time in seconds. Time zero represents the point just before the potential was stepped to -1.51 V.
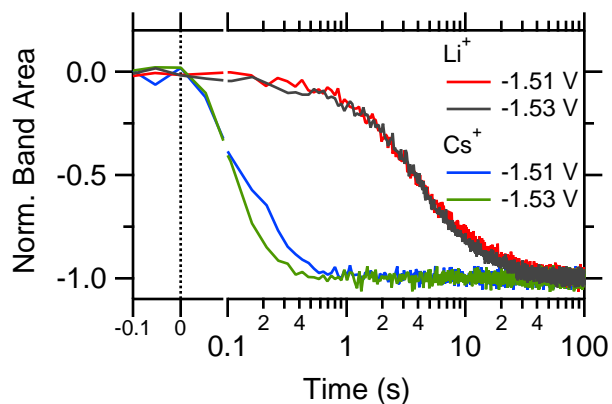
Fig. S 8: Comparison of the traces of the normalized integrated band areas of linearly-bonded CO following a step from the potential at saturation coverage of -1.04 V vs. SHE to a reduction potential of -1.51 V or -1.53 V. The normalization constants for the Li^+ data are 409 and 405 mOD cm^{-1} for final potentials of -1.51 and -1.53 V, respectively. The normalization constants for the Cs^+ data are 366 and 360 mOD cm^{-1} for final potentials of -1.51 and -1.53 V, respectively. For each electrolyte, the experiment at the more negative reduction potential was carried out on the same film just after completion of the first jump to -1.51 V. Both experiments give virtually identical integrated band areas, demonstrating that the film is stable during these experiments.
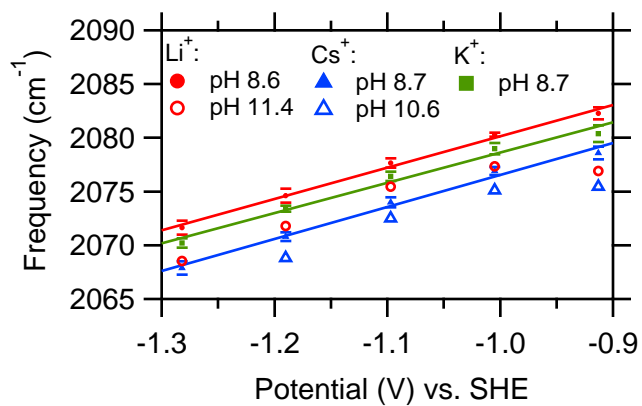
Fig. S 9: CO peak frequency shift vs. applied potential for different cations and pH* values. Solid symbols represent the average of three independent experiments carried out on freshly deposited Cu films in $MDCO_3$ electrolytes. Hollow symbols represent the average of two experiments carried out on freshly deposited Cu films in M_2CO_3 electrolytes.
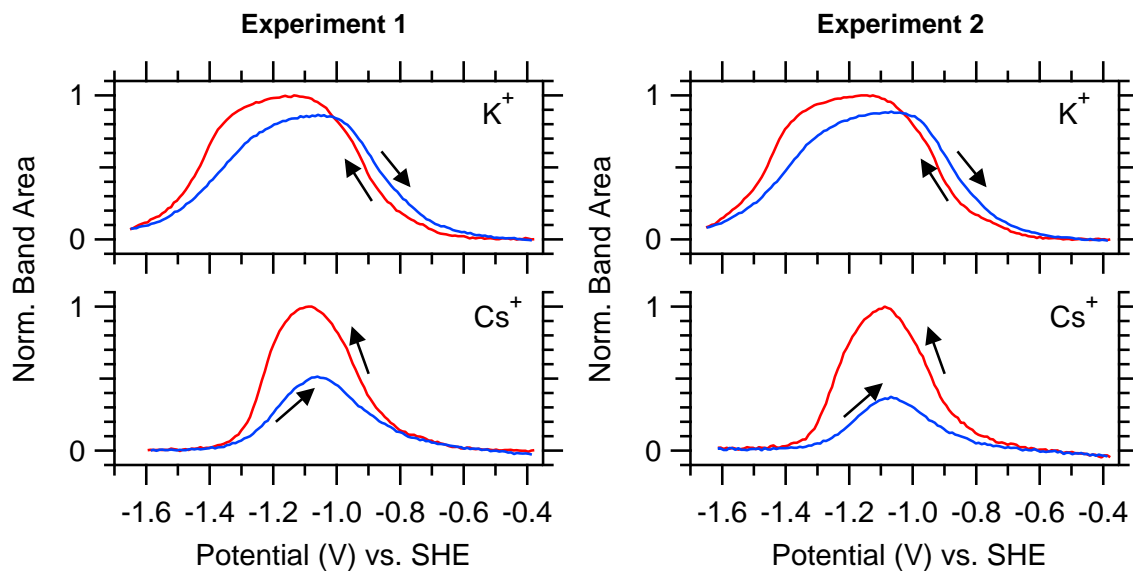
Fig. S 10: Normalized integrated band areas of linearly-bonded CO as a function of applied potential in CO-saturated 0.05 M alkali carbonates as indicated. The figure shows the data for two independent experiments carried out for each cation. The normalization constants for Experiment 1 are 407 and 405 mOD cm^{-1} for Li$^+$ and Cs$^+$, respectively. The normalization constants for Experiment 2 are 471 and 464 mOD cm^{-1} for Li$^+$ and Cs$^+$, respectively.

Experiment 1

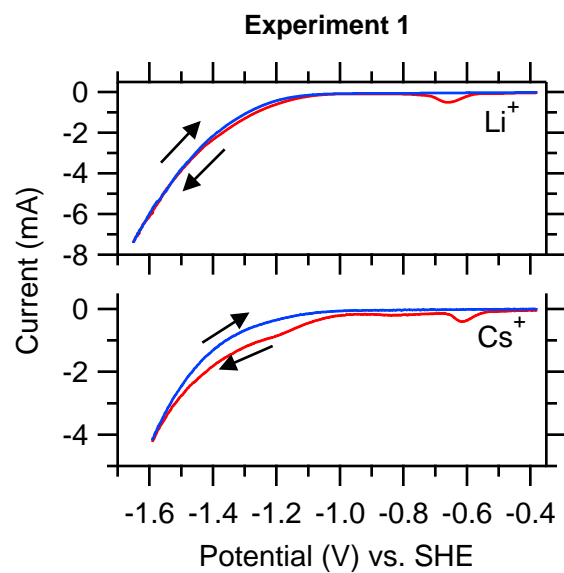Current (mA) vs. Potential (V) vs. SHE

Li$^+$

Cs$^+$

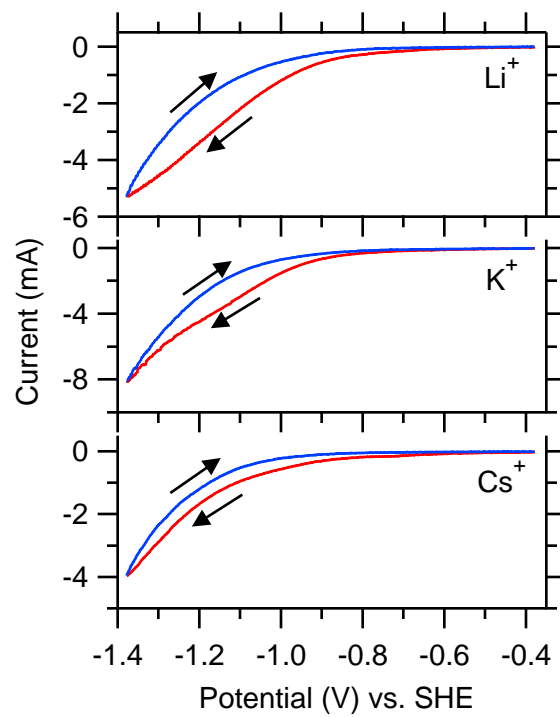Fig. S 11: Cyclic voltammetric current-voltage curves for Experiment 1 in Fig. S10.

Fig. S 12: Cyclic voltammetric curves for data presented in Fig. 6 (CO_2-purged electrolyte) of the main text.
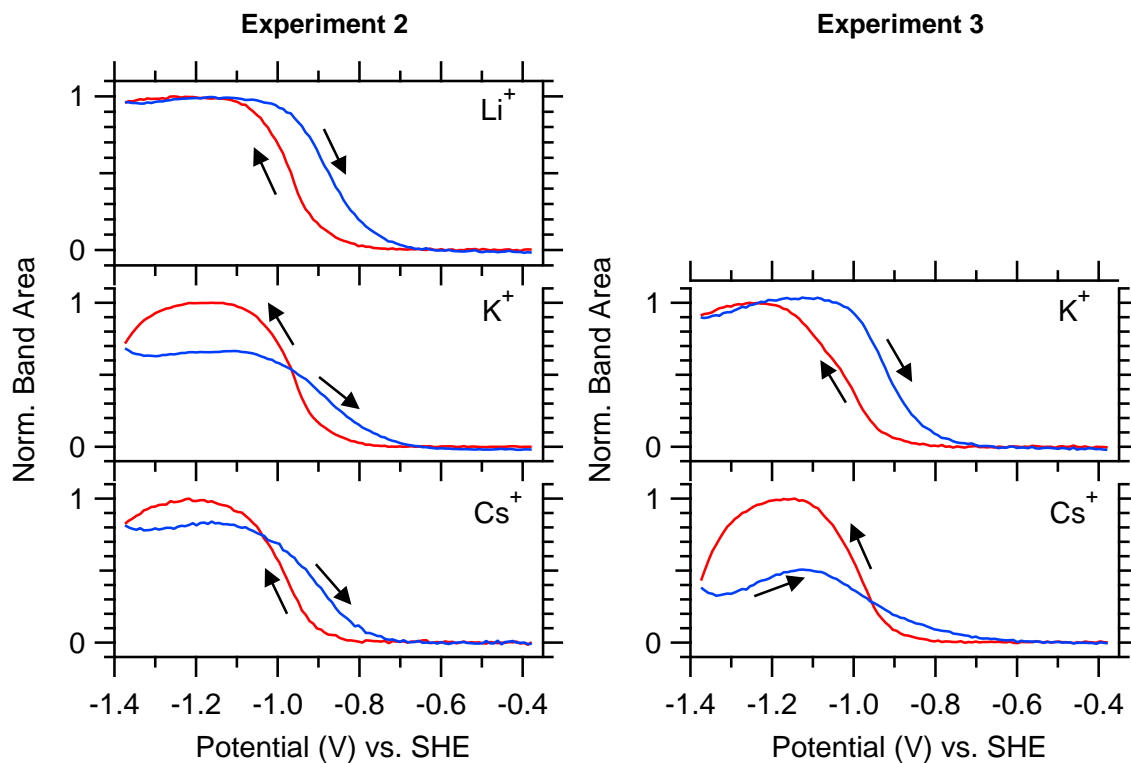
Fig. S 13: Normalized integrated band areas of linearly-bonded CO as a function of applied potential for two additional experiments for K^+ and Cs^+ and 1 additional experiment for Li^+ in CO_2-saturated 0.1 M alkali metal bicarbonates. The normalization constants for Experiment 2 are 559, 573, and 315 mOD cm^{-1} for Li^+, K^+, and Cs^+, respectively. The normalization constants for Experiment 3 are 417 and 469 mOD cm^{-1} for K^+, and Cs^+, respectively. The normalization constants for the experiment of the main text (Fig. 6) are 600, 425, and 438 mOD cm^{-1} for Li^+, K^+, and Cs^+, respectively.
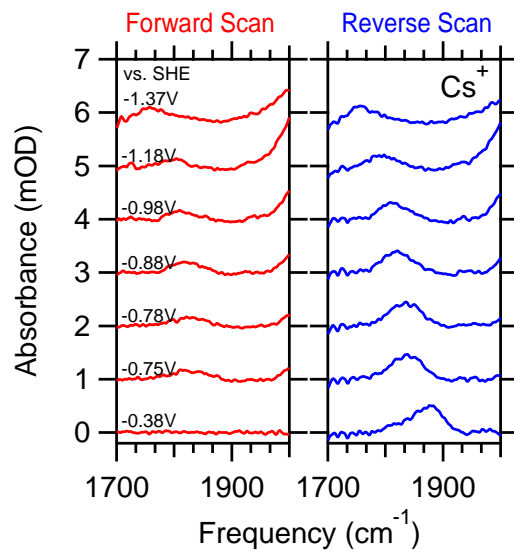
Fig. S 14: Representative IR spectra in the region of multiply-bonded CO as a function of applied potential in CO-saturated 0.1 M CsDCO$_3$.

References

(1) Wang, H.-F.; Yan, Y.-G.; Huo, S.-J.; Cai, W.-B.; Xu, Q.-J.; Osawa, M. *Electrochim. Acta* **2007**, *52*, 5950–5957.

(2) Wuttig, A.; Liu, C.; Peng, Q.; Yaguchi, M.; Hendon, C. H.; Motobayashi, K.; Ye, S.; Osawa, M.; Surendranath, Y. *ACS Cent. Sci.* **2016**, *2*, 522–528.

(3) Gunathunge, C. M.; Li, X.; Li, J.; Hicks, R. P.; Ovalle, V. J.; Waegele, M. M. *J. Phys. Chem. C* **2017**, *121*, 12337–12344.

(4) Waszczuk, P.; Zelenay, P.; Sobkowski, J. *Electrochim. Acta* **1995**, *40*, 1717 – 1721.